Characterization of Bifacial Photovoltaic Modules Based on I-V Curves Outdoor Measurement

Alberto Dolara, Sonia Leva, Domenico Mazzeo, Emanuele Ogliari
Department of Energy
Politecnico di Milano
Milan, Italy
{alberto.dolara, sonia.leva, domenico.mazzeo, emanuelegiovanni.ogliari}@polimi.it

***Abstract*—Photovoltaic (PV) systems are well known for their simplicity of design, environmental friendliness, and low maintenance. Among the PV technologies, the behaviour of bifacial PV modules was studied in this research. Measurements of the I-V curves were carried out in the SolarTech^{LAB} test facility at the Department of Energy of Politecnico di Milano, Italy, to detect the bifacial PV module behaviour, mainly in terms of power performance. In particular, I-V and power-voltage curves were measured at different tilt angles to consider several irradiance and cell temperature levels with both sides uncovered as well as with the back side covered. This last configuration was tested to evaluate the contribution of the rear face in the overall photoelectric conversion process. The comparison between the bifacial and monofacial operations highlighted that the power at the maximum power point of the bifacial operation can increase up to 13%. At the same time, leaving the rear face free allows for reducing the bifacial cell temperature up to about 6°C.**

***Index Terms*—Photovoltaic, I-V Curve, Monofacial PV module, Bifacial PV module**

I. Introduction

The social and governmental interest in cleaner technologies meeting energy needs while complying with environmental regulations is growing. Governments are promoting and supporting environmentally friendly and renewable energy sources, creating legislation for their support and promotion. Among them, the 2030 Agenda [1] and Paris Agreement [2] are the most important actions. This new energy approach opens up a huge market for clean technologies and this paves the way for international investment and competition. Photovoltaic (PV) can be considered one of the most developed and widespread renewable energy generating systems to reduce the impact of climate change, which in turn affects PV performance [3].

Bifacial PV modules (bPV) represent an effective technology capable of increasing electricity generation since they convert solar radiation into electrical energy reaching both their front and rear side. Compared to monofacial PV (mPV) cells, the structure of bPV cells is based on a photoelectric conversion layer on both sides of the crystalline silicon substrate: the front layer is designed to convert global irradiance - that is the sum of beam, sky-diffuse and ground-reflected components - while the rear layer is designed to convert the irradiance that is the results of ground albedo and light reflection by nearby objects [4]. Moreover, bPV technology makes use of high-performance PV cells with multiple busbars to improve electron collection by the electrodes and to reduce the series resistance, hence increasing the PV cell efficiency. The *Bifacial Gain* (BG) quantifies the increase in power performance of bPV modules, representing the relative increase of the energy yield of a bPV module compared to an mPV module.

The comparison among mPV and bPV modules is based on their I-V (Current-Voltage) curve and the resulting P-V (Power-Voltage) curve. Their determination is fundamental to knowing the PV modules' power performance in different weather and installation conditions beforehand. The reference standard, defining the procedures for the measurement of the I-V characteristics of bPV devices in natural or simulated sunlight and applicable to either single PV cells, sub-assemblies of such cells or entire PV modules, is the IEC TS 60904-1-2:2019 [5]. Liang et al. revised the standard IEC 60904-1-2 with the aim of: (i) quantifying the backside reflections of bPV modules when the front side irradiance is at 1000 W/m^2 and (ii) demonstrating some of the metrological challenges associated with meeting the target specified by the standard, as well as the importance of selecting a non-reflective material behind the side not illuminated [6]. To fully define the I-V curve of bPV modules under Standard Test Conditions (STC), it is necessary to extend the definition of STC to include spectral distribution and total irradiance on the rear side of the PV module. As a general rule, indoor PV module characterization allows for the most precise control of these quantities. A simple method involves measuring each side of the bPV module separately with a single light source and keeping the other side in the dark, covered with a non-reflecting black sheet. An approach for characterizing bPV modules for the front and the rear side illumination was presented by Singh et al. [7]. Instead, Schmid et al. compared different measurement methods to characterize bPV modules with the front side only and bifacial illumination [8]. In addition, a comparison between single-sided and bifacial illumination was made. To contribute to this research development, this work aims to study the power performance behaviour of the

This study was partly conducted within the Agritech National Research Center and received partial funding from the European Union Next-GenerationEU (PIANO NAZIONALE DI RIPRESA E RESILIENZA (PNRR) – MISSIONE 4 COMPONENTE 2, INVESTIMENTO 1.4 – D.D. 1032 17/06/2022, CN00000022). This manuscript reflects only the authors' views and opinions, neither the European Union nor the European Commission can be considered responsible for them. All authors have contributed equally.

979-8-3503-4743-2/23/$31.00 ©2023 IEEE

bPV module in different weather and operating conditions. In particular, the purposes are:

- The determination of the bPV module power performance for different solar irradiance and PV cell temperature values, highlighting their importance and their influence. Changes in these operating parameters were obtained by regulating the tilt angle, as well as measuring the I-V curve on different days and periods.
- The comparison between the power performance of the same bPV module operated with both faces uncovered and with the rear face covered, namely with only the front face generating electrical energy. This comparison allows highlighting the contribution of the rear face on the power performances. The irradiance on the bPV module, and consequently the bPV cell temperature, were changed by varying the relevant tilt angle.

In all the operating conditions, an analysis of the main parameters, such as the short circuit current and open circuit voltage, was carried out.

II. Materials and Methods

The purpose of this research is to collect and analyze the I-V curves that characterize the operation and the performance of bPV modules under different weather and operating conditions, namely for (i) bPV and mPV configurations and (ii) different tilt angles, days and periods, thus different irradiance and PV cell temperature values. Specifically, the bPV module was located in Milan at the SolarTech^{LAB} (latitude 45.50°N; longitude 9.16°E), placed on the building roof of the Department of Energy of Politecnico di Milano. The layout of the SolarTech^{LAB} and the instrumentation available were designed and improved over the years to measure the performance of a PV system integrated into external shading devices [9], to assess the performance of organic PV modules in real outdoor conditions [10], [11], to test PV modules and maximum power point tracking under dynamical partial shading conditions [12]–[14], to investigate the effects of PV modules early degradation [15], and to provide real data for the assessment between different forecasting methods (deterministic models and a hybrid method based on artificial neural network) for the day-ahead output power [16].

The solar incidence angle on the bPV module surface was changed by a variable-tilt structure that allows the rotation of the bPV module only on its lateral axis; the structure azimuth angle is -6°(assuming that 0°is the South direction and angles increase towards the West). In this way, in addition to varying the solar irradiance on the front and back of the bPV module, some insights can be gained regarding the optimal tilt angle of the bPV modules, as is usually done for conventional mPV modules [17]. Experimental campaigns were performed under sunny days and stable irradiance as required by the IEC 60904-1-2. The sheet to cover the back side of the PV module was made of cardboard coated on the outer side with an aluminum layer that allows keeping the irradiance on the rear surface lower than 3(W/m^2), as prescribed by the IEC 60904-1-2.

A. Bifacial PV characteristics and working conditions

The PV module taken into consideration is a 3S DUAL 72N model (3SBA345A) manufactured by Enel Green Power[1]. Its main ratings are reported in Table I.

TABLE I: bPV module ratings in STC

Dimensions	1983 x 998 mm	**Cell number**	72
I_{sc}	9.18 A	I_{sc} **temp. coeff.**	+0.048 $\%/°C$
V_{oc}	47.9 V	V_{oc} **temp. coeff.**	-0.3 $\%/°C$
P_{mpp}	345 W	P_{mpp} **temp. coeff.**	-0.38 $\%/°C$
V_{mpp}	39.3 V	**Efficiency**	17.4 %
I_{mpp}	8.78 A	**Bifaciality factor**	>85 %

Two different bPV operating conditions were considered: the first one, hereafter referred to as *bifacial operation*, corresponds to both uncovered; the second one, hereafter referred to as *monofacial operation*, consists of covering cardboard on the back side, with so only the front side can generate power. Fig. 1 represents the two operating configurations.

(a) (b)

Fig. 1: bPV module configured for *bifacial operation* (1a) and *monofacial operation* (1b).

B. Instrumentation

To perform the experimental campaign a specific instrumentation was required. In particular:

- The environmental conditions are measured with a meteorological station, including sensors for global and diffuse irradiances on the horizontal plane, wind speed and direction sensors, temperature and humidity sensors, and rain collector [18].
- The I-V curve tracer, which is based on a capacitor charging circuit and a network analyzer for the simultaneous sampling of the current and the voltage at the bPV module terminals. As a result of the resistance of the current loop, the scanning voltage range is between a few volts (depending on the short circuit current) and the open circuit voltage.
- Thermocouples, together with their reading and acquisition system, register the temperature of the back side of the bPV module.

To determine all irradiance components at a tilt angle β for both the front and back side of the bPV module, two different well-known models were employed: the Liu and Jordan [19] and the View Factor models [20].

[1]https://www.enelgreenpower.com/content/dam/enel-egp/documenti/pannelli-fotovoltaici-hjt/EGP_Datasheet_HJT.pdf [Accessed February 20, 2023]

TABLE II: Experimental campaigns

Campaign	**1**st	**2**nd	**3**rd
Date	17/05/2022	26/05/2022	06/06/2022
Tilt angle (°)	0 30 45 60	0 20 40 60 90	0 30 45 60
Tilt setups	4	5	4
Front **Back**	uncovered uncovered	uncovered uncovered	uncovered covered
Samples	3	2	2
Events	5	5	5

C. Experimental campaigns

Before the beginning of the test campaigns, both the sides of the bPV module were accurately cleaned and the thermocouples were placed on the rear side of the bPV module. Then, the tilt angle was set and PV module thermal steady state condition was reached: the I-V curve measurement cycle started as soon as the temperatures were stable. This procedure was repeated every time the tilt angle was changed. Every I-V curve measurement cycle collects the data corresponding to five I-V curves assumed to be scanned at the same irradiance and PV cells temperature, as the whole set of I-V curves was measured within a time range of a few tens of seconds. In the post-processing, an I-V curve was excluded in case the irradiance corresponding to the same I-V curve differs more than 2% from the mean irradiance of the group. For each tilt angle, more I-V curve measurement cycles under similar conditions are repeated to get a more robust data set. In summary, for each bPV operating condition, three cycles, each consisting of five events, were taken. To obtain a unique I-V curve for each measurement cycle and tilt angle, the closest I-V curve to the mean I-V curve of the group was identified. The representative I-V curve corresponding to a specific tilt angle was identified by determining the I-V curve characterized by the global irradiance on the front side of the bPV module closest to the mean global irradiance of the whole set of 15 I-V curves detected for a specific tilt angle.

Three experimental campaigns, as reported in Table II, were performed. Each campaign consists of several I-V measurement cycles. Some tilt angles were tested, and for each of them, a 5-minute waiting time was introduced between each cycle of I-V curve measurement at the same tilt angle. Campaigns 1 (17^{th} May) and 2 (26^{th} May) were focused on the effect of irradiance on the bPV power performance, and Campaign 3 (6^{th} June) was focused on the contribution of the rear side to the electrical energy generation.

III. Results

The raw data from the three experimental campaigns were processed to determine:

- the irradiance components on the front and rear sides of the bPV module,
- the mPV and bPV cell temperatures,
- the electrical main parameters of the I-V curve.

TABLE III: 1^{st} campaign: irradiance components, cell temperature and main electrical parameters

Tilt angle (°)	**0**	**30**	**45**	**60**
$G_b^F\ (W/m^2)$	849	914	827	697
$G_d^F\ (W/m^2)$	85	94	87	83
$G_r^F\ (W/m^2)$	0	6	12	21
$G^F\ (W/m^2)$	933	1014	926	801
$G_d^R\ (W/m^2)$	0	7	15	28
$G_r^R\ (W/m^2)$	88	81	72	63
$G^R\ (W/m^2)$	88	88	87	91
T_c	49.6	53.6	54.1	55.2
$V_{oc}\ (V)$	42.6	42.5	42.2	42.4
$I_{sc}\ (A)$	9.01	10.21	9.51	8.67
$P_{mpp}\ (W)$	287.1	318.7	294.0	273.5
$V_{mpp}\ (V)$	33.6	33.5	33.5	33.6
$I_{mpp}\ (A)$	8.54	9.51	8.78	8.14

TABLE IV: 2^{nd} campaign: irradiance components, cell temperature and main electrical parameters

Tilt angle (°)	**0**	**20**	**40**	**60**	**90**
$G_d^F\ (W/m^2)$	582	632	642	575	312
$G_d^F\ (W/m^2)$	172	170	154	137	95
$G_r^F\ (W/m^2)$	0	2	9	19	41
$G^F\ (W/m^2)$	754	803	805	731	448
$G_d^R\ (W/m^2)$	0	5	20	46	95
$G_r^R\ (W/m^2)$	71	69	65	58	41
$G^R\ (W/m^2)$	71	74	85	104	136
$T_c\ (C)$	45.8	48.1	49.7	50.0	45.2
$V_{oc}\ (V)$	43.6	43.5	43.3	43.1	43.0
$I_{sc}\ (A)$	7.45	8.18	8.40	7.84	5.08
$P_{mpp}\ (W)$	246.8	269.1	273.0	254.8	172.7
$V_{mpp}\ (V)$	35.4	35.4	34.1	34.8	35.4
$I_{mpp}\ (A)$	6.97	7.59	8.00	7.33	4.88

The representative I-V curves and the corresponding P-V curves for each operating condition of the three test campaigns are shown in Fig. 2, 3 and 4, while the corresponding irradiance data and main electrical parameters are reported in Table III, IV and V. In these tables, the superscripts F and R refer to the front and rear side of the bPV module, while the subscripts b, d and r identify the plane of the array beam, sky-diffuse and ground-reflected irradiance components, respectively.

A. First experimental campaign

As regards the 1^{st} campaign, characterized by high levels of irradiance, the following considerations can be highlighted:

- The power at the maximum power point shows a bell curve as a function of the tilt angle, in the same way as the front side solar irradiance. It is maximized for a tilt angle between β = 30°÷45° with a maximum value of 318.7 W for β = 30°, obtained with a solar irradiance on the front and back side of 1014 W/m^2 and 88 W/m^2, respectively. The current at the maximum power follows the same trend as the maximum power as a function of the tilt angle, while the voltage at the maximum power is almost constant.

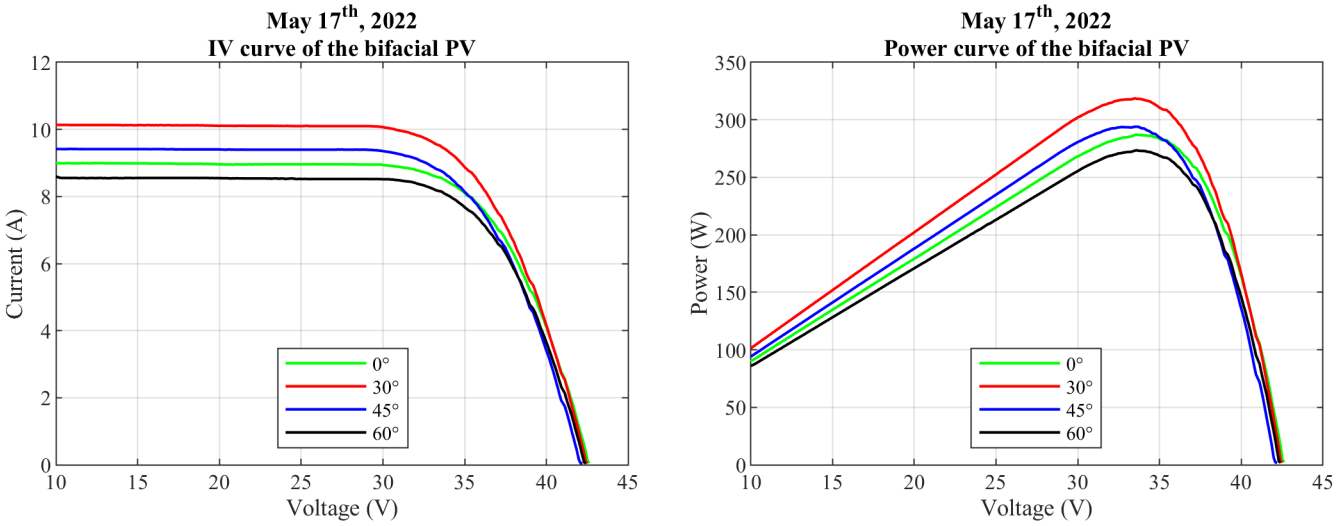

Fig. 2: I-V and power curves of the first campaign.

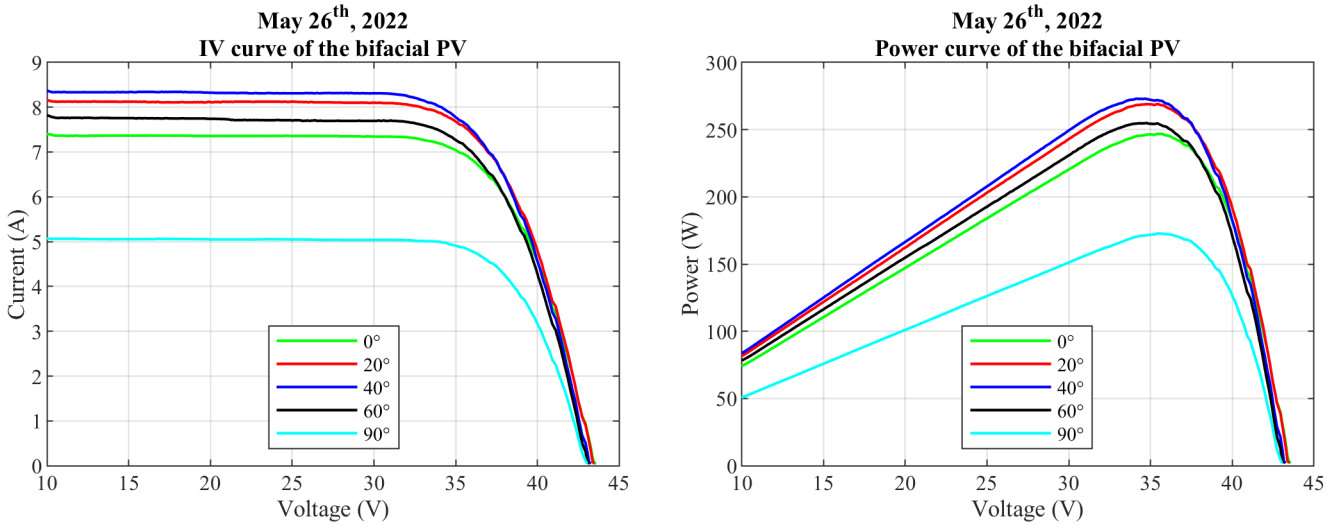

Fig. 3: I-V and power curves of the second campaign.

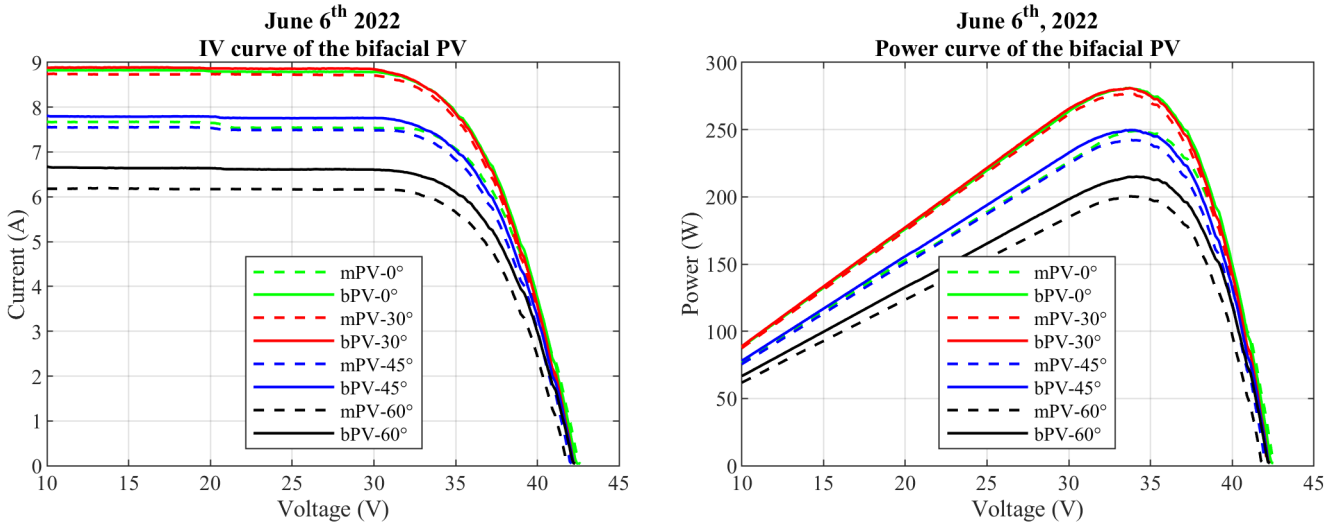

Fig. 4: I-V and power curves of the third campaign.

TABLE V: 3^{rd} campaign: irradiance components, cell temperature and main electrical parameters

PV configuration	**mPV**				**bPV**			
Tilt angle (°)	0	30	45	60	0	30	45	60
$G_b^F\ (W/m^2)$	709	801	691	546	793	783	687	544
$G_d^F\ (W/m^2)$	75	81	72	60	93	76	72	61
$G_r^F\ (W/m^2)$	0	5	12	19	0	5	12	19
$G^F\ (W/m^2)$	784	888	774	625	886	864	771	624
$G_d^R\ (W/m^2)$	0	0	0	0	0	5	12	20
$G_r^R\ (W/m^2)$	0	0	0	0	83	74	67	58
$G^R\ (W/m^2)$	0	0	0	0	83	80	79	78
$T_c\ (C)$	54.3	59.8	58.9	57.2	54.0	56.4	55.9	53.2
$V_{oc}\ (V)$	42.6	42.3	42.1	41.9	42.5	42.3	42.3	42.3
$I_{sc}\ (A)$	7.72	8.77	7.59	6.23	8.88	8.92	7.91	6.70
$P_{mpp}\ (W)$	249.0	277.0	242.4	200.4	281.0	280.8	249.7	215.0
$V_{mpp}\ (V)$	34.1	33.5	33.6	33.8	33.7	33.7	33.8	34.1
$I_{mpp}\ (A)$	7.29	8.27	7.21	5.92	8.34	8.33	7.38	6.30

- The lowest maximum power corresponds to a tilt angle of β = 60°. In this configuration, the solar irradiance on the front and back side are 801 W/m^2 and 91 W/m^2, respectively, leading to a maximum power of 273.5 W.
- The solar irradiance on the back side is almost constant with the tilt angle. Overall, it is about 10% of the front solar irradiance.
- The cell temperature grows with the tilt angle and it ranges between 49.6 °C and 55.2 °C. This result is mainly correlated with both the irradiance on the front side of the bPV module and the ambient temperature.
- The short circuit current I_{sc} is directly proportional to the irradiance and shows the same trend of the current at the maximum power point. The highest short circuit current corresponds to β = 30° and it is 10.21 A.
- The open circuit voltage V_{oc} is almost constant and ranges between 42.4 V and 42.6 V.

B. Second experimental campaign

Concerning the 2^{th} campaign, characterized by medium-low levels of irradiance, the same qualitative results of the 1^{st} campaign were found, as reported in Fig. 3 and Table IV. The differences are only quantitatively and they can be summarized as follows:

- The power at the maximum power point is maximized for a tilt angle between β = 20°÷40° with a very low variation in this range; the maximum value of 273.0 W for β = 40° corresponds to a solar irradiance on the front and back side of 805 W/m^2 and 85 W/m^2, respectively.
- The lowest maximum power corresponds to a tilt angle of β = 90°. In this configuration the solar irradiance on the front and back side are 448 W/m^2 and 136 W/m^2, respectively, leading to a maximum power of 172.7 W.
- The solar irradiance on the back side increases with the tilt angle, especially at tilt angles higher than β = 60°. As the tilt angle increases, the sky-diffuse irradiance on the back of the module increases and the ground-reflected irradiance decreases. Since the floor of the test facility is a metal grate and its albedo is very low, the intensity of ground-reflected irradiance is lower than the intensity of sky-diffuse irradiance.
- The cell temperature is higher for high irradiance values and it ranges between 45.2 °C and 50.0 °C. This result is mainly correlated with the irradiance on the bPV module front side, but it is also affected by the irradiance on the bPV rear side and the ambient temperature.
- The maximum value of the I_{sc} is 8.40 A for β = 40°, while V_{oc} is almost constant and ranges between 43.0 V and 43.6 V.

C. Third experimental campaign

Concerning the third campaign, the outcomes are slightly affected by the time required to perform tests; small irradiance variations were found between the first and the last I-V curve measurement at the same tilt angle. For both *monofacial operation* and *bifacial operation*, the maximum power was found for β = 30°. Instead, the comparison between the bPV module configured for *monofacial operation* and configured for *bifacial operation* at the same tilt angle highlights a more evident contribution of the rear face to the electricity generation as the irradiance on the front side reduces. In particular, in the *bifacial operation*, an increase in the maximum power of 13%, 1%, 3% and 7% is obtained, respectively, with the four tilt angles considered in the range β = 0°÷60°. Excluding the case of tilt equal to 0° due to the large difference in the front side irradiance between the tests in the two configurations, the highest increase in power is detected for the tilt angle corresponding to the minimum front side irradiance. The irradiance on the front side mainly depends on the angle of incidence of the beam irradiance component and, therefore, on the tilt angle, while the irradiance on the back side is almost constant as it is given by the sum of sky-diffuse and ground-reflected irradiance, whose values as a function of the tilt angle tend to compensate. For any tilt angle, except for β = 0° because of the same reason discussed above, the PV cell temperature of the bPV module configured for *bifacial operation* is lower than the PV cell temperature of the bPV module configured for *monofacial operation*. The cardboard added to configure the bPV module for *monofacial operation* reduces the natural convection on the rear side and increases the overall thermal

TABLE VI: Solar efficiency

Tilt angle (°)		0	20	30	40	45	60	90
First campaign		0.142	/	0.146	/	0.147	0.155	/
Second campaign		0.151	0.155		0.155	/	0.154	0.150
Third campaign	mPV	0.161	/	0.158	/	0.158	0.162	/
	bPV	0.147	/	0.150	/	0.148	0.155	/

resistance of the module. The highest difference corresponds to the lowest irradiance on the front side of the bPV module.

To make comparable all tests, the solar efficiency, defined as the ratio of the power at the maximum power point to the overall solar power incident on the front and back sides of the PV module, was calculated. Table VI summarizes the solar efficiency obtained for all tilt angles and operating conditions of the PV module. It is evident that, for the bPV module, the highest solar efficiency is obtained for tilt angles greater than the optimal tilt angle. In the 2^{nd} campaign, the efficiency is higher compared to the first one because of the lower temperatures detected, despite the lower levels of irradiance. For the 3^{rd} campaign, the solar efficiency of the bPV module configured for *bifacial operation* is lower than the one configured for the *monofacial operation*. For the *monofacial operation*, the maximum efficiency is achieved for tilt angles far from the one maximizing the output power. These results demonstrate that the efficiency of the photoelectric conversion on the two bPV module sides is different and the front side is more efficient than the rear side.

IV. Conclusion

The experimental I-V and power curves of the bPV module detected in this research are strongly affected by irradiance on both sides of the bPV module and the resulting bPV cells temperature, which were modified by means of a tilt angle variation. In particular, during the experimental analysis, the maximum power was found for a tilt angle of around 30° for all campaigns and bPV module operating conditions. The short-circuit current and the current at the maximum power as a function of the tilt angle follow the same trend of the maximum output power, while the open-circuit voltage and the voltage at the maximum power are almost constant with the tilt angle. The comparison between the *bifacial operation* and the *monofacial operation* highlighted an increase of the maximum power ranging betwenn 1% and 13%, as a function of the climatic conditions, due to the contribution of the rear face to the overall photoelectric conversion process. The determination of the solar efficiency demonstrated that the photoelectric conversion process on the front side is more efficient than the same process on the rear side. Although the difference in power output due to the contribution of the rear side is small, the amount of energy yield is significant in large-scale PV systems, making the adoption of bPV modules feasible in terms of installation, operation, and maintenance.

References

[1] O. Cf, "Transforming our world: the 2030 agenda for sustainable development," *United Nations: New York, NY, USA*, 2015.

[2] Y. Gao, X. Gao, and X. Zhang, "The 2 c global temperature target and the evolution of the long-term goal of addressing climate change—from the united nations framework convention on climate change to the paris agreement," *Engineering*, vol. 3, no. 2, pp. 272–278, 2017.

[3] N. Matera, D. Mazzeo, C. Baglivo, and P. M. Congedo, "Will climate change affect photovoltaic performances? a long-term analysis from 1971 to 2100 in italy," *Energies*, vol. 15, no. 24, p. 9546, 2022.

[4] R. Guerrero-Lemus, R. Vega, T. Kim, A. Kimm, and L. Shephard, "Bifacial solar photovoltaics – a technology review," *Renewable and Sustainable Energy Reviews*, vol. 60, pp. 1533–1549, 2016. [Online]. Available: https://www.sciencedirect.com/science/article/pii/S1364032116002768

[5] I. E. Commission *et al.*, "Photovoltaic devices-part 1-2: Measurement of current-voltage characteristics of bifacial photovoltaic (pv) devices," *IEC TS*, pp. 60 904–1.

[6] T. S. Liang, D. Poh, and M. Pravettoni, "Challenges in the pre-normative characterization of bifacial photovoltaic modules," *Energy Procedia*, vol. 150, pp. 66–73, 2018.

[7] J. P. Singh, A. G. Aberle, and T. M. Walsh, "Electrical characterization method for bifacial photovoltaic modules," *Solar energy materials and solar cells*, vol. 127, pp. 136–142, 2014.

[8] A. Schmid, G. Dülger, G. Baraah, U. Kräling, and F. Ise, "Iv measurement of bifacial modules: bifacial vs. monofacial illumination," *Proc. 33rd EUPVSEC, Amsterdam, The Netherlands*, vol. 1624, 2017.

[9] E. Piccoli, A. Dama, A. Dolara, and S. Leva, "Experimental validation of a model for pv systems under partial shading for building integrated applications," *Solar Energy*, vol. 183, pp. 356–370, 2019.

[10] A. Dolara, G. di Fazio, S. Leva, G. Manzolini, R. Simonetti, and A. Terenzi, "Outdoor assessment and performance evaluation of opv modules," *IEEE Journal of Photovoltaics*, vol. 11, no. 2, pp. 391–399, 2021.

[11] L. Hanne, A. Dolara, and S. Leva, "Performance and thermal analysis of organic photovoltaic modules in outdoor conditions," 2022.

[12] A. Dolara, G. C. Lazaroiu, S. Leva, and G. Manzolini, "Experimental investigation of partial shading scenarios on pv (photovoltaic) modules," *Energy*, vol. 55, p. 466 – 475, 2013.

[13] M. Aghaei, A. Dolara, F. Grimaccia, S. Leva, D. Kania, and J. Borkowski, "Experimental comparison of mppt methods for pv systems under dynamic partial shading conditions," in *EEEIC 2016 - International Conference on Environment and Electrical Engineering*, 2016.

[14] A. Dolara, S. Leva, G. Magistrati, M. Mussetta, E. Ogliari, and R. V. Arvind, "A novel mppt algorithm for photovoltie systems under dynamic partial shading-recurrent scan and track method," in *2016 IEEE International Conference on Renewable Energy Research and Applications, ICRERA 2016*, 2016.

[15] A. Dolara, S. Leva, G. Manzolini, and E. Ogliari, "Investigation on performance decay on photovoltaic modules: Snail trails and cell microcracks," *IEEE Journal of Photovoltaics*, vol. 4, no. 5, p. 1204 – 1211, 2014.

[16] E. Ogliari, A. Dolara, G. Manzolini, and S. Leva, "Physical and hybrid methods comparison for the day ahead pv output power forecast," *Renewable energy*, vol. 113, pp. 11–21, 2017.

[17] N. Matera, D. Mazzeo, C. Baglivo, and P. M. Congedo, "Hourly forecasting of the photovoltaic electricity at any latitude using a network of artificial neural networks," *Sustainable Energy Technologies and Assessments*, vol. 57, p. 103197, 2023.

[18] K. A. K. Niazi, T. Kerekes, A. Dolara, Y. Yang, and S. Leva, "Performance assessment of mismatch mitigation methodologies using field data in solar photovoltaic systems," *Electronics*, vol. 11, no. 13, p. 1938, 2022.

[19] B. Y. Liu and R. C. Jordan, "The interrelationship and characteristic distribution of direct, diffuse and total solar radiation," *Solar Energy*, vol. 4, no. 3, pp. 1–19, 1960. [Online]. Available: https://www.sciencedirect.com/science/article/pii/0038092X60900621

[20] J. Appelbaum, "The role of view factors in solar photovoltaic fields," *Renewable and Sustainable Energy Reviews*, vol. 81, pp. 161–171, 2018. [Online]. Available: https://www.sciencedirect.com/science/article/pii/S1364032117310924